

MRI in the assessment of congenital heart disease

Aparna Deshpande, MBBS, MRCP, FRCR

Cardiac magnetic resonance imaging (MRI) plays a vital role in the investigation and follow up of patients with congenital heart disease both in terms of anatomical and functional analysis.¹ Congenital heart disease (CHD) has a prevalence of about 0.9%. Over the last several decades the overall survival of individuals with an underlying CHD has improved dramatically from 20% to about 90% of individuals reaching adulthood.² This improvement results from better surgical techniques, medical treatments and percutaneous intervention for later complications.

Various noninvasive imaging investigations for follow up include echocardiogram (TTE and TEE) and cardiac MRI. Cardiac computed tomography (CT) is increasingly being utilized, particularly when cardiac MRI is contraindicated, such as in those patients with a pacemaker or defibrillator.³ However, CT employs ionizing radiation.

Dr. Deshpande is a Consultant Cardiothoracic Radiologist at Glenfield Hospital, University Hospitals of Leicester, Leicester, England.



This article reviews the basic image sequences routinely used in imaging CHD (Table 1). It also demonstrates various imaging findings of the most common congenital heart pathologies.

Patient preparation

It is important to ensure the patient is not claustrophobic. Younger patients may require sedation; general anesthesia and a dedicated anesthetic team may be needed for the duration of the scan in children to ensure a safe airway and assess the patient. If there are any

devices or pacemakers present, confirmation should be made that these are MRI conditional.¹

The ECG trace is used to synchronize the cardiac cycle with cine image acquisition. Retrospective ECG gating is performed throughout the cardiac cycle over several heartbeats if the heart rate is regular. Arrhythmia rejection may be used if there is an occasional ectopic beat. Prospective ECG gating is used if there is underlying arrhythmia. There is a trigger delay from the R wave and the images are obtained over a set acquisition

Table 1. Routine cardiac MRI sequences

- Spin echo sequence (HASTE images) for anatomy
- Standard gradient echo (GE) cine: 4, 3, 2 chamber cine SSFP acquisition. Other sequences performed include LVOT (left ventricular outflow tract), aortic valve views, RVOT view and pulmonary valve view
- Short axis cine gradient echo SSFP stack: Left ventricular analysis
- Axial cine gradient echo SSFP stack: Right ventricular analysis
- Gadolinium (Gd) enhanced high resolution MR angiogram and time resolved MR angiogram
- Velocity encoded phase contrast cine imaging: Analysis of peak velocity and flow analysis through valves, vessels and conduit
- Navigator: imaging of the heart, thoracic vasculature and heart
- Late gadolinium enhancement (LGE) images: To assess for fibrosis and infarct

window. Scanning in end diastole may be missed resulting in underestimation of volumes and function.^{4,5}

Sequences and techniques

HASTE

This is a spin echo sequence also referred to as black blood imaging. Anatomical assessment is useful with HASTE images.^{1,5} This sequence has lower SNR (signal to noise) than the gradient echo sequence, although it is less prone to cardiac and respiratory motion due to rapid imaging.⁴ This acquisition is performed in the axial plane, but additional views in sagittal and coronal planes can be performed. Visceral position, atrioventricular and ventricular-arterial concordance can be evaluated. Systemic and pulmonary venous return as well as position of the aortic arch can be determined. The HASTE sequence is also useful to assess for extracardiac abnormalities.²

Standard gradient echo cine imaging

Gradient echo cine images are obtained using spoiled gradient echo pulse sequences or SSFP sequences.⁵ The standard views are four, three and two chamber views, LVOT and aortic valve cine views.⁴ These sequences allow initial visual assessment of the ventricles,

atria and valves. Short axis cine views are performed to assess the left ventricle.^{1,3} Similarly, an axial cine view or 4-chamber stack view can be performed to assess the right ventricle.¹ Ventricular volumes and systolic function can also be analyzed on the short axis and axial cine stack views. Additional sequences assessing the right ventricle include pulmonary valve cine and RVOT cine views.⁴

Contrast-enhanced (CE) MR angiogram

Gadolinium-enhanced MR angiography plays a crucial role in assessing vasculature structures. Gadolinium-based contrast reduces the T1 time of blood, improving contrast between the blood pool and surrounding tissues.⁶ It has high spatial resolution and 3D reconstructions may be performed.^{6,7} Conditions such as aortic coarctation and Marfan's syndrome may require aortic angiography. The pulmonary vasculature is assessed in Tetralogy of Fallot (TOF) and follow up of surgically corrected transposition of the great arteries (TGA). In single ventricle pathology, angiography is performed to assess circulation and a Fontan circuit, if present. Time-resolved CE MR angiogram is used for sequential assessment as the contrast passes

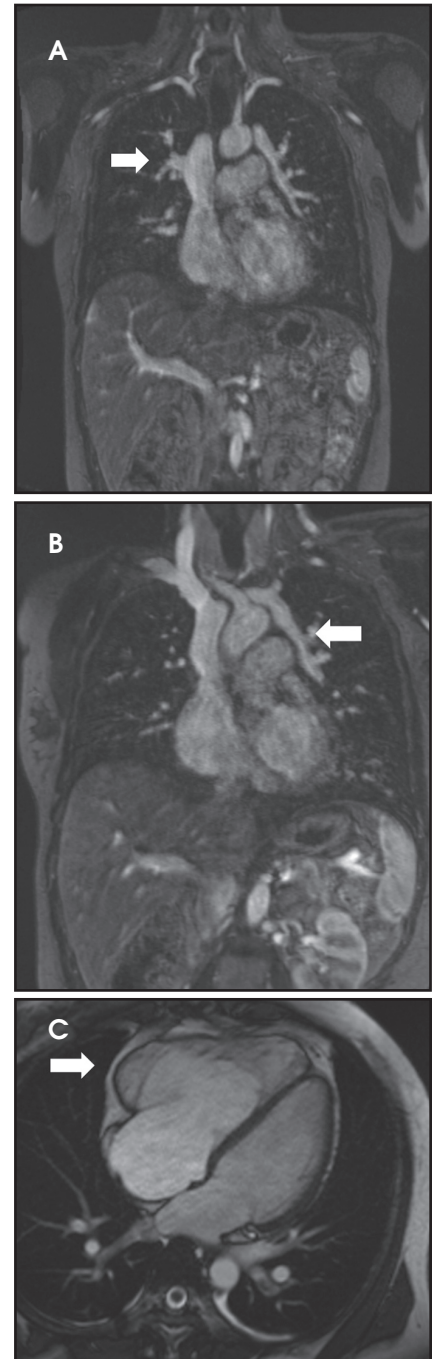


FIGURE 1. (A) This 32-year-old woman had ASD closure as a child but persistent PAPVR caused right ventricular dilatation. The right upper lobe pulmonary vein is seen to drain into the SVC (arrow). (B) The left upper lobe pulmonary vein is seen to drain into the left brachiocephalic vein (arrow). (C) The right ventricle (arrow) is seen to be severely dilated (EDV 187 mL/m²) compared to the left (EDV 81 mL/m²) on this 4-chamber SSFP gradient echo sequence. The Qp:Qs flow ratio is calculated at 1.89:1.0. There is no residual ASD.

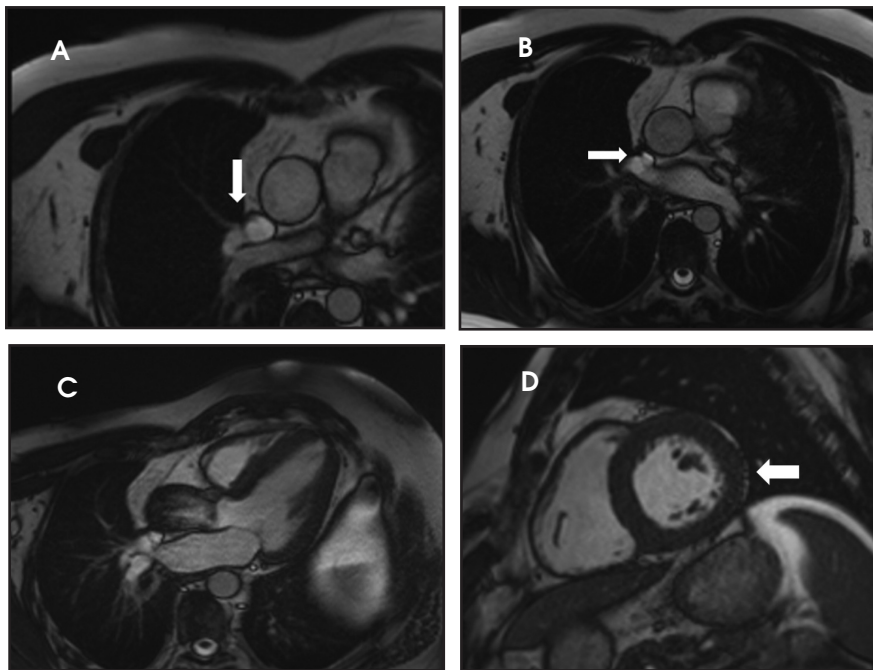


FIGURE 2. (A) The right upper lobe pulmonary vein drains into the SVC (arrow). (B) Suggestion of connection of SVC to the left atrium in keeping with sinus venosus ASD (arrow). (C) The three-chamber SSFP gradient echo sequence shows flow acceleration across the aortic valve in keeping with aortic stenosis and a peak velocity of 4.2 m/s. (D) There is concentric left ventricular hypertrophy (arrow) on this short axis gradient echo SSFP sequence.

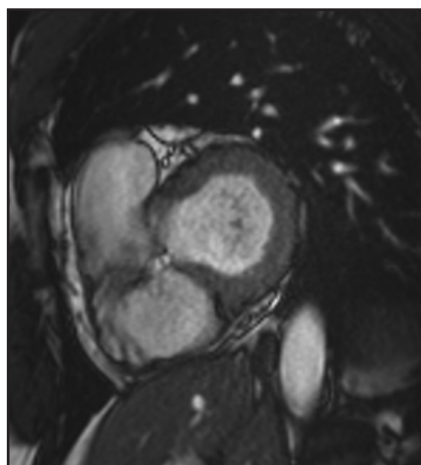


FIGURE 3. The perimembranous VSD is appreciated on this short axis SSFP gradient echo sequence.

through the vasculature and to assess for collaterals and pulmonary arteriovenous malformations.^{2,7}

Velocity encoding phase contrast cine imaging (VEPC imaging)

This technique can be performed to assess peak velocity across a valve or regurgitant fraction using “through plane” phase contrast cine imaging.¹ In-plane

cine imaging is used to assess the direction of blood flow, which is particularly important in septal defects.⁸ The ascending aorta, aortic valve, pulmonary valve and branch pulmonary arteries are assessed with these sequences. Shunt fraction can be calculated by assessing forward flow in the main pulmonary (Qp) and ascending aorta (Qs). A Qp:Qs of 1.5:1.0 indicates a significant shunt, resulting in elevated right heart pressures and pulmonary hypertension.

Navigator sequence

This technique is a balanced SSFP acquisition used to obtain anatomical information. A T2 preparation increases signal of the blood compared to myocardium. The sequence is triggered to end diastole to avoid cardiac motion. A navigator is used to monitor diaphragmatic movement and avoid respiratory motion artefact. The scan may be performed without contrast, however administration of Gd-based contrast improves the SNR and CNR (contrast to noise ratio).⁷ It may be used to cover the entire heart and assess vasculature. Often it is used to

assess the origins and proximal course of the coronary arteries.

LGE imaging

These sequences are used for assessment of fibrosis or infarction. This is normally performed 10-20 minutes following administration of 0.1-0.2 Mmol/kg Gd-based contrast. The LGE sequences used are the segmented double inversion recovery sequence; the phase sensitive inversion recovery (PSIR), or the single shot acquisition. An initial inversion pulse is used to null the myocardium (TI time).⁷ A PSIR sequence is less sensitive to a suboptimal TI time.⁹ A single shot acquisition can be performed within a single R-R interval; however, this has a lower SNR and CNR¹⁰ compared to segmented images. Fibrosis may act as a substrate for arrhythmia. Enhancement may be seen if there has been surgical patch repair, scar from previous surgery or postsurgical infarction.⁶

Spectrum of cardiac anomalies

Atrial septal defects (ASD)

Atrial septal defects constitute the most common shunt lesion detected de novo in adulthood.¹¹ Secundum ASD is the most common type (50-70%), while primum ASD¹² is less common at 15-30% and is often associated with defect of the atrioventricular valve.¹¹ Sinus venosus and coronary sinus defects are rare (Figures 1 and 2). Cardiac MRI plays an important role in assessing and quantifying right ventricular overload, visualizing the defect and calculating the shunt fraction. En face phase contrast cine imaging allows measurement of the defect.¹² By the 5th decade about 75% of patients suffer from exertional dyspnea.¹³ Elevated right ventricular volumes and a shunt fraction (Qp:Qs) of 1.5:1.0 is an indication for ASD closure¹² by surgery or percutaneous means. Following ASD closure, cardiac MRI is important to assess for any residual shunting, the degree of reduction in right ventricular volumes and for assessment of complications such as device dislodgement.

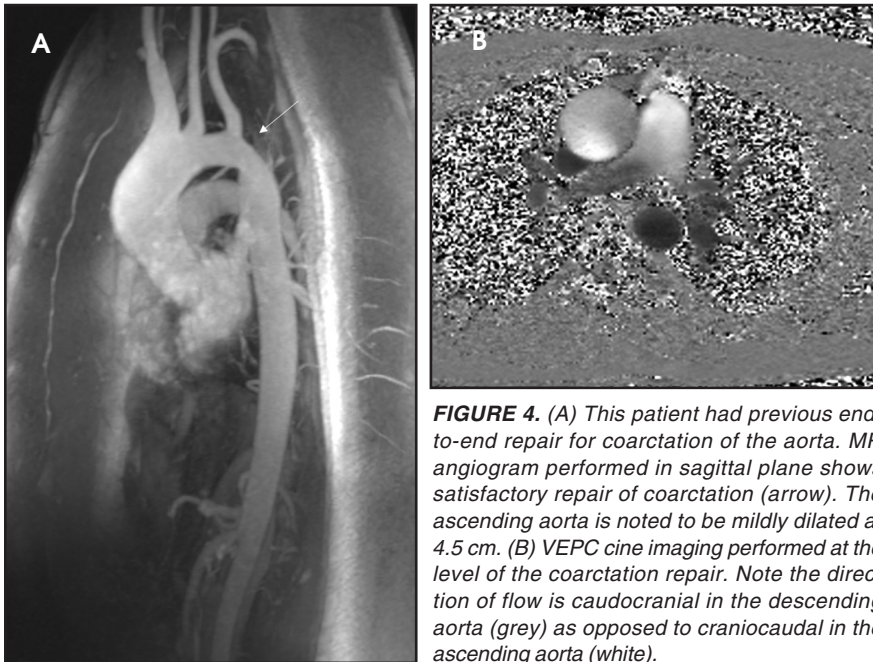


FIGURE 4. (A) This patient had previous end-to-end repair for coarctation of the aorta. MR angiogram performed in sagittal plane shows satisfactory repair of coarctation (arrow). The ascending aorta is noted to be mildly dilated at 4.5 cm. (B) VEPC cine imaging performed at the level of the coarctation repair. Note the direction of flow is caudocranial in the descending aorta (grey) as opposed to craniocaudal in the ascending aorta (white).

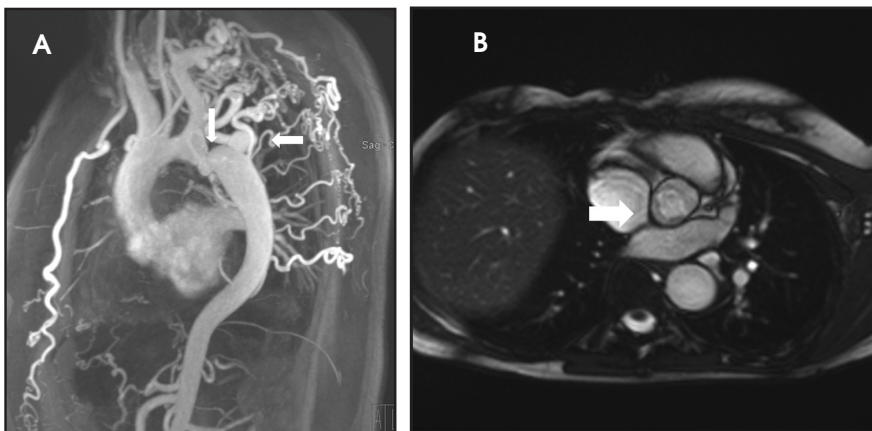


FIGURE 5. (A) 25-year-old man with diagnosis of previously undetected coarctation of the aorta. The vertical arrow points to the site of narrowing distal to the origin of the left subclavian artery. The horizontal arrow points to an aneurysmal collateral arising just distal to the coarctation site. Further extensive collaterals noted. The patient subsequently had a stent placed across the coarctation site with good outcome. (B) The aortic valve gradient echo sequence in this patient demonstrates a bicuspid valve (arrow).

Ventricular septal defects (VSD)

Ventricular septal defects are the most common CHD, making up 20% of congenital heart anomalies. They may be associated with TOF, TGA and atrioventricular canals.¹² There is an increased association with Down's, DiGeorge's¹⁴ and Turner's syndromes. They may be muscular, inlet, outlet or membranous VSD. About 80% are membranous VSDs, while 20% are muscular VSD.¹¹ Membranous VSDs occur just under the aortic valve at the level of the tricuspid

valve (Figure 3). The septal leaflet of the tricuspid valve may close the defect or the aortic cusp may prolapse into the defect.¹² It may be associated with aortic or tricuspid regurgitation. Cardiac MRI has a vital role in assessing the defect, quantifying ventricular volumes and the shunt fraction.

Coarctation of aorta

Coarctation occurs at the junction of the distal aortic arch with the descending thoracic aorta. It can occur due to

protrusion of tissue extending from the posterior aspect of the aortic wall to the opposite wall, contiguous with the ductus arteriosus.¹⁵ Coarctation may be associated with other conditions, such as Turner's syndrome and bicuspid aortic valve,¹⁶ and accounts for 5% of CHD.¹⁷

Surgical management includes resection and end-to-end repair, subclavian flap repair, prosthetic patch aortoplasty, interposition graft or extra-anatomic bypass graft.¹⁷ Late complications include recurrent coarctation and pseudo-aneurysm at the repair site.¹⁷ Cardiac MRI is useful to assess location and severity of the coarctation, as well as the peak flow velocity. Collateral flow can be assessed by quantifying flow just proximal to the coarctation and in the descending aorta at the level of the hiatus.¹⁸ The aortic valve can be assessed for morphology and stenosis or regurgitation. Aortic angiogram is obtained to assess the coarctation site, collaterals and remainder of the thoracic aorta¹⁷ (Figures 4, 5). The aortic arch may be hypoplastic. Left ventricular hypertrophy¹⁶ due to coarctation or aortic valve stenosis may be visualized on the SSFP cine sequences.

Tetralogy of Fallot (TOF)

TOF is the commonest of the cyanotic congenital cardiac conditions and consists of a perimembranous VSD (80%), subpulmonary infundibular stenosis, overriding aorta and right ventricular hypertrophy (RVH). Right-sided aortic arch may occur in 25% of cases.¹⁹ Management in infancy includes closure of the VSD with RVOT muscle resection (infundibulectomy), transannular patch or right ventricle-to-pulmonary artery conduit. Infundibulectomy is performed when there is moderate RVOT obstruction in the presence of a normal pulmonary valve annulus.¹⁹ A transannular patch is performed when there is associated pulmonary valve stenosis (Figure 6).²⁰ Complications include chronic pulmonary regurgitation and right ventricle dilatation.¹⁹ A right ventricle-to-pulmonary artery valved conduit is performed when there is pulmonary atresia, which constitutes the most severe form of

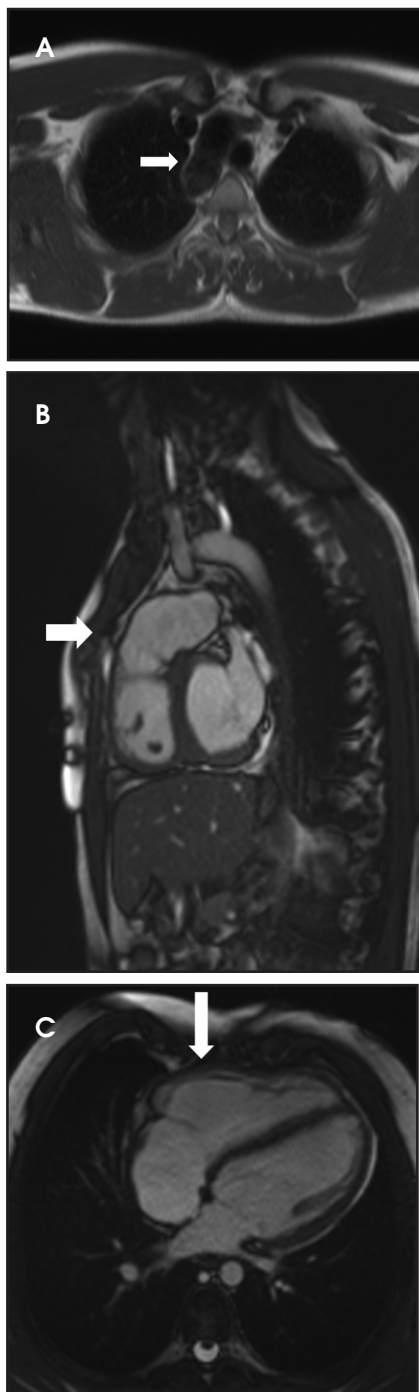


FIGURE 6. (A) Patient with previous transannular patch repair for Tetralogy of Fallot. The HASTE sequence reveals a right-sided aortic arch (arrow). (B) This patient had transannular patch repair for TOF. The RVOT SSFP gradient echo sequence reveals an aneurysmal RVOT. (C) The four-chamber SSFP gradient sequence reveals the right ventricle is dilated compared to the left. On quantification, the right ventricle was dilated to EDV 151 ml/mm² compared to the left ventricle (EDV 91 ml/mm²).

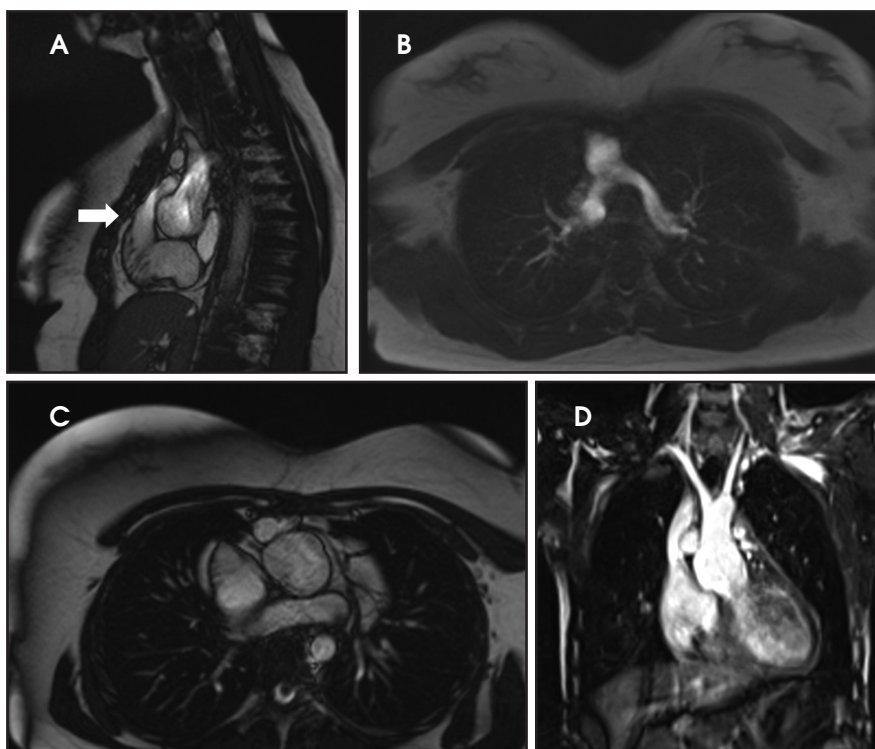


FIGURE 7. (A) Patient had arterial switch surgery for transposition of great arteries. This view demonstrates flow acceleration across the pulmonary valve (arrow). The neo-aorta posteriorly is noted to be dilated. (B) The MR pulmonary angiogram demonstrates the branch pulmonary arteries passing on either side of the nonopacified ascending aorta. (C) The aortic valve SSFP gradient echo sequence demonstrates the pulmonary valve anterior to the aortic valve in keeping with the arterial switch surgery. Dilated aortic root noted. (D) Navigator sequence of the whole heart demonstrates a dilated aortic root. The branch pulmonary arteries are seen on both side of the ascending aorta.

TOF.¹⁹ Late complications include conduit degeneration with stenosis or regurgitation.

About 2-5% patients may have a residual VSD.²⁰ Recurrent or residual pulmonary stenosis may occur in the RVOT, at the level of the pulmonary valve or branch pulmonary arteries.² Left ventricular dysfunction is a late complication due to poor ventriculo-ventricular interaction.²⁰ Tricuspid regurgitation may be seen in 10% cases.¹⁹

Pulmonary valve replacement or percutaneous pulmonary valve implantation (PPVI) is considered when the right ventricular end diastolic volume is greater than 150 mL/m² with impaired RV ejection fraction less than 47%.²¹

MRI sequences include RVOT cine SSFP sequences which demonstrate the transannular patch with bulging and akinesis of the aneurysmal patch. In infundibulectomy, the RVOT is of nor-

mal size and contractility on cine images unless there are complication such as RVOT stenosis.²⁰ The right ventricle to pulmonary artery conduit and pulmonary regurgitation are also visualized in this sagittal view. Contrast-enhanced MR angiogram can be used to assess dimensions of the pulmonary arteries and thoracic aorta. 3D reconstructions may be performed for PPVI work up. Flow analysis of the valves and across conduit and branch pulmonary arteries can be performed with VE PC cine imaging. LGE sequences will show enhancement around transannular patch repair due to formation of fibrosis.²⁰

Transposition of great arteries (TGA)

This entity represents about 5% of all CHD.²² In D-TGA, there is atrioventricular (AV) concordance with ventriculoarterial (VA) discordance. The

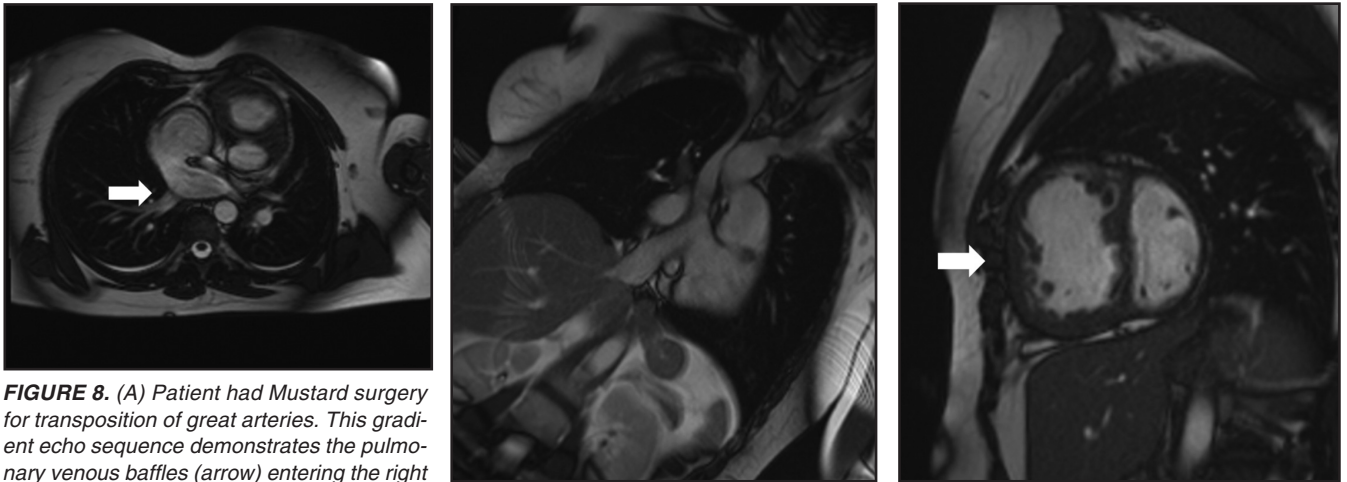


FIGURE 8. (A) Patient had Mustard surgery for transposition of great arteries. This gradient echo sequence demonstrates the pulmonary venous baffles (arrow) entering the right atrium. (B) This view demonstrates the superior and inferior baffles draining into the left ventricle (C) On this short axis gradient sequence the right ventricle is dilated and hypertrophied (arrow) as it is functioning as the systemic ventricle. Note the D-shaped left ventricle. The septum is straightened due to elevated right heart volume and pressure.

aorta arises from the right ventricle via a subaortic infundibulum while the pulmonary artery arises directly from the left ventricle.² This is associated with other abnormalities, including VSD, in 50% of cases. Pulmonary outflow tract obstruction and aortic coarctation occur in about 5% cases.²³ TGA is one of the common forms of cyanotic heart disease, and initial management can include atrial septostomy to treat the initial cyanosis.²² Subsequent surgery options include Mustard/Senning baffles, arterial switch or Rastelli surgery.

Arterial switch is performed when there is an intact ventricular septum. This was first performed by Jatene.²² The 20-year survival is nearly 90%.²² The aorta and pulmonary artery are transected above the level of the valve sinuses. The pulmonary trunk is moved forward into a new position anterior to the aorta and the great arteries are sutured in place. The coronary arteries are sutured into the neo-aorta. The aorta and pulmonary artery are transected above the level of the valve sinuses. The pulmonary trunk is moved forward into a new position anterior to the aorta and the great arteries are sutured in place. Coronary arteries are sutured into the neo-aorta. Long-term complications include supra-valvular pulmonary outflow obstruction, neo-aortic regurgitation and arrhythmias. Branch pulmonary artery steno-

sis may occur at a rate of 1% per year (Figure 7).²

A Rastelli procedure is performed when there is a subaortic VSD and pulmonary VSD.²³ The VSD is utilized as part of the LVOT to direct blood from the left ventricle to the aorta. The pulmonary valve is oversown and a conduit placed between the right ventricle and pulmonary artery. Complications include PA-RVOT conduit degeneration and stenosis.²³ In atrial switch surgery or a Mustard–Senning procedure, VA discordance is maintained. Venous baffles direct deoxygenated venous blood to the pulmonary artery via the left ventricle. The pulmonary venous baffles allow circulation of oxygenated blood through the right ventricle to the aorta.²³ Superior venous baffle obstruction occurs in 5–10% of cases.²⁴ Baffle leak is more common than baffle obstruction. These are seen more easily with transoesophageal echocardiogram rather than with cardiac MRI²³ (Figure 8). Right heart dysfunction and tricuspid regurgitation may develop.² Pulmonary hypertension occurs in 7% of cases.²³ Arrhythmia is a cause for sudden death.²⁵

Cardiac MRI is important to assess biventricular and valvular function with SSFP gradient echo sequences. Neo-aortic dilatation and regurgitation can be assessed. Branch pulmonary artery stenosis can be evaluated with CE angiogram and peak velocity

calculated with VEPC imaging. Baffle leaks and obstruction can be detected. The oblique coronal view is used to assess systemic baffles while the oblique axial plane is used to assess pulmonary venous baffle.² With severe SVC baffle obstruction, a dilated azygous system can be sought. In baffle leaks, Qp:Qs can be measured with phase contrast cine imaging to calculate shunt fraction.²⁵ LGE images provide an indicator of systemic RV failure following atrial switch repair.²⁶ The RV to PA conduit in the Rastelli is best seen with sagittal oblique SSFP sequences or turbo spin echo images. To assess stenosis, an SSFP gradient echo sequence will demonstrate the dephasing jet through the site of obstruction. VEPC cine imaging can be performed to assess peak velocity and regurgitant fraction.²⁵ The Navigator sequence may be used to assess anatomy and origin of the coronary arteries.

Conclusion

Cardiac MRI has a vital role in CHD follow up. It allows accurate anatomical and functional assessment. The workup for potential surgery or percutaneous procedures may also be performed with the help of cardiac MRI. This article has highlighted some of the commonest noncyanotic and cyanotic conditions requiring regular follow up with cardiac MRI.

REFERENCES

1. Fratz S, Chung T, Greil GF, et al. Guidelines and protocols for cardiovascular magnetic resonance in children and adults with congenital heart disease: SCMR expert consensus group on congenital heart disease. *J Cardiovasc Magn Reson*. 2013;15(1):51. doi:10.1186/1532-429X-15-51.
2. Babar JL, Jones RG, Hudsmith L. Application of MR Imaging in Assessment and Follow-up of Congenital Heart Disease in Adults. *Radiographics*. 2010;11-24. doi:10.1148/rg.e40/-/DC1.
3. Kilner PJ, Geva T, Kaemmerer H, Trindade PT, Schwittler J, Webb GD. Recommendations for cardiovascular magnetic resonance in adults with congenital heart disease from the respective working groups of the European Society of Cardiology. *Eur Heart J*. 2010;31(7):794-805. doi:10.1093/eurheartj/ehp586.
4. Ginat DT, Fong MW, Tuttle DJ, Hobbs SK, Vyas RC. Cardiac imaging: Part 1, MR pulse sequences, imaging planes, and basic anatomy. *Am J Roentgenol*. 2011;197(4):808-815. doi:10.2214/AJR.10.7231.
5. Ridgway JP. Cardiovascular magnetic resonance physics for clinicians: part I. *J Cardiovasc Magn Reson*. 2010;12(1):71. doi:10.1186/1532-429X-12-71.
6. Buechel ERV, Grosse-Wortmann L, Fratz S, et al. Indications for cardiovascular magnetic resonance in children with congenital and acquired heart disease: An expert consensus paper of the Imaging Working Group of the AEPC and the Cardiovascular Magnetic Resonance Section of the EACVI. *Eur Heart J Cardiovasc Imaging*. 2015;16(3):281-297. doi:10.1093/ehjci/jeu129.
7. Biglinds J, Radjenovic A, Ridgway JP. Cardiovascular magnetic resonance physics for clinicians: part II. *J Cardiovasc Magn Reson*. 2012;14(1):66. doi:10.1186/1532-429X-12-71.
8. Srichai MB, Lim RP, Wong S, Lee VS. Cardiovascular applications of phase-contrast MRI. *Am J Roentgenol*. 2009;192(3):662-675. doi:10.2214/AJR.07.3744.
9. Badalà F, Nouri-mahdavi K, Raoof DA. NIH Public Access. *Computer (Long Beach Calif)*. 2008;144(5):724-732. doi:10.1038/jid.2014.371.
10. Wildgruber M, Settles M, Herrmann K, Beer AJ, Rummeny EJ, Huber AM. Inversion-recovery single-shot cardiac MRI for the assessment of myocardial infarction at 1.5 T with a dedicated cardiac coil. *Br J Radiol*. 2012;85(1017). doi:10.1259/bjr/57965172.
11. Wang ZJ, Reddy GP, Gotway MB, Yeh BM, Higgins CB. Cardiovascular Shunts: MR Imaging Evaluation 1. *RadioGraphics*. 2003;23(suppl_1):S181-S194. doi:10.1148/rg.23si035503.
12. Rajiah P, Kanne JP. Cardiac MRI: Part 1, Cardiovascular Shunts. 2011;(October):603-620. doi:10.2214/AJR.10.7257.
13. Teo KSL, Disney PJ, Dundon BK, et al. Assessment of atrial septal defects in adults comparing cardiovascular magnetic resonance with transthoracic echocardiography. *J Cardiovasc Magn Reson*. 2010;12:44. doi:10.1186/1532-429X-12-44.
14. McElhinney DB, Driscoll D a, Levin ER, Jawad AF, Emanuel BS, Goldmuntz E. Chromosome 22q11 deletion in patients with ventricular septal defect: frequency and associated cardiovascular anomalies. *Pediatrics*. 2003;112(6):e472. doi:10.1542/peds.112.6.e472.
15. Karaosmanoglu AD evrim, Khawaja RD eedar A, Onur MR uhi, Kalra MK. CT and MRI of aortic coarctation: pre- and postsurgical findings. *AJR Am J Roentgenol*. 2015;204(3):W224-W233. doi:10.2214/AJR.14.12529.
16. Kimura-Hayama ET, Meléndez G, Mendizábal AL, Meave-González A, Zambrana GFB, Corona-Villalobos CP. Uncommon congenital and acquired aortic diseases: role of multidetector CT angiography. *Radiographics*. 2010;30(1):79-98. doi:10.1148/rg.301095061.
17. Konen E, Merchant N, Provost Y, McLaughlin PR, Crossin J, Paul NS. Coarctation of the Aorta before and after Correction: The Role of Cardiovascular MRI. *Am J Roentgenol*. 2004;182(5):1333-1339. doi:10.2214/ajr.182.5.1821333.
18. Hom JJ, Ordovas K, Reddy GP. Velocity-encoded cine MR imaging in aortic coarctation: functional assessment of hemodynamic events. *Radiographics*. 2008;28(2):407-416. doi:10.1148/rg.282075705.
19. Norton KI, Tong C, Glass RBJ, Nielsen JC. Cardiac MR Imaging Assessment Following Tetralogy of Fallot Repair. *Radiographics*. 2006;26:197-211. doi:10.1148/rg.261055064.
20. Ordovas KG, Muzzarelli S, Hope MD, et al. Cardiovascular MR Imaging after Surgical Correction of Tetralogy of Fallot: Approach Based on Understanding of Surgical Procedures. *Radiographics*. 2013;33(4):1037-1052. doi:10.1148/rg.334115084.
21. Geva T. Repaired tetralogy of Fallot: the roles of cardiovascular magnetic resonance in evaluating pathophysiology and for pulmonary valve replacement decision support. *J Cardiovasc Magn Reson*. 2011;13(1):9. doi:10.1186/1532-429X-13-9.
22. Villafañe J, Lantin-Hermoso MR, Bhatt AB, et al. D-transposition of the great arteries: The current era of the arterial switch operation. *J Am Coll Cardiol*. 2014;64(5):498-511. doi:10.1016/j.jacc.2014.06.1150.
23. Warnes CA. Transposition of the great arteries. *Circulation*. 2006;114(24):2699-2709. doi:10.1161/CIRCULATIONAHA.105.592352.
24. Kammeraad JAE, Van Deurzen CHM, Sreeram N, et al. Predictors of sudden cardiac death after mustard or senning repair for transposition of the great arteries. *J Am Coll Cardiol*. 2004;44(5):1095-1102. doi:10.1016/j.jacc.2004.05.073.
25. Lu JC, Dorfman AL, Attili AK. Evaluation with Cardiovascular MR Imaging of Baffles and Conduits Used in Palliation or Repair of Congenital Heart Disease 1. 2012. doi:10.1148/rg.323115096/-/DC1.
26. Ntsinjana HN, Hughes ML, Taylor AM. The role of cardiovascular magnetic resonance in pediatric congenital heart disease. *J Cardiovasc Magn Reson*. 2011;13:51. doi:10.1186/1532-429X-13-51.